Coastal Dynamics 2017
Paper No. 006

RAPID CHANGE IN COASTAL MORPHOLOGY DUE TO SAND-BYPASSING CAPTURED BY UAV-BASED MONITORING SYSTEM

Yoshinao Matsuba[1], Shinji Sato[2] and Keiji Hadano[3]

Abstract

A UAV-based monitoring system was developed and applied to Asaba Coast in Japan, where a new pipeline-based sand-bypassing system was introduced and beach recovery is expected near the outlet. The monitoring system was composed of two sub-systems; the estimation of submarine bathymetry by using extraction of wave crest-lines and the estimation of subaerial topography by using SfM (Structure from Motion) technique. Field measurements were conducted seasonally for about one year, while shoreline monitoring was also conducted with surveillance cameras during the same period. The monitoring system was found to be capable of quantifying quick beach recovery around the outlet, and therefore considered to be a powerful tool to evaluate the performance of the sand-bypassing system.

Key words: sand-bypassing, nearshore bathymetry monitoring, image analysis, UAV, Structure from Motion, shoreline change

1. Introduction

Significant beach erosion is developed on the Enshu-nada Coast, in Shizuoka Prefecture, Japan. The erosion is caused by natural and anthropogenic impacts, such as high waves, tides and construction of dams and harbors. The erosion is especially significant near the Fukude-Asaba Coast, where the longshore sand transport is blocked by the breakwater of the Fukude Harbor, resulting excessive deposition on the upstream (west) side and severe erosion propagated on the Asaba Coast located on the downstream (east) side. In order to solve the problem, the Shizuoka Prefectural government introduced an automated sand bypassing system through a pipeline in 2015, with extensive surveys of successful experiences on Gold Coast in Australia (Tweed Sand Bypassing, 2017). By using this system, sand is collected by hydraulic jet pumps installed at a pier constructed on the west side of the Fukude Harbor and is transported to the eroding Asaba Coast through a 2 km pipeline (see Figure 1). The capacity of the system is designed at 80 thousand cubic meter per year. The effectiveness of the bypassing system must be evaluated by continuous monitoring of waves, currents and topography surveys. However, it is difficult to conduct frequent monitoring with appropriate resolutions both in time and space because conventional bathymetry surveys are time consuming and require laborious works. On the Fukude-Asaba Coast, nearshore bathymetry surveys are conducted for cross-sectional profiles only once or twice in a year with interval of hundreds of meters. It is important to monitor the impact given by this new system with high resolution in both time and space in order to understand the effectiveness.

Frequent estimations of nearshore topography can be achieved by using surveillance cameras based on image analysis. Lippmann and Holman (1989) developed a new technique to map underlying sand bars by using time averaged images. As a more quantitative method, Stockdon and Holman (2000), Liu et al. (2012) developed a method to estimate water depth based on the wave celerity captured by surveillance cameras. These image-based monitoring systems appear to have potentials to contribute to low-cost high-resolution nearshore monitoring. It is noted however that the analysis is restricted by the coverage of cameras. Therefore, it is considered that using surveillance cameras for nearshore monitoring must be

[1]Postgraduate Student, Dept. Of Civil Eng., The University of Tokyo, Japan. matsuba@coastal.t.u-tokyo.ac.jp
[2]Proffessor, ditto, sato@coastal.t.u-tokyo.ac.jp
[3]Postgraduate Student,ditto, cagekez14@coastal.t.u-tokyo.ac.jp

complemented by more flexible tools.

As a new tool realizing frequent and flexible monitoring, the use of Unmanned Aerial Vehicle (UAV) has been introduced in recent years. Inukai et al. (2015) utilized UAV in order to monitor rip currents from the high altitude. Mancini et al. (2013) applied SfM (Structure from Motion) method, which is used to build three-dimensional model from pictures taken from multiple angles, to estimate subaerial topography of beach by using pictures taken by UAV. Bathymetry estimation by UAV was also developed by Matsuba and Sato (2017). Even though these application of UAV to the monitoring suggested the effectiveness of using UAV, the practical cases where UAV was applied were so few that more verification of its effectiveness must be done.

Based on the situation mentioned above, in this study, a UAV based monitoring system was developed and applied to the Asaba Coast, where rapid topography change is expected near the outlet of the sand bypassing system. The monitoring system is composed of two sub-systems; the estimation of submarine bathymetry by using extraction of wave crest lines and the estimation of subaerial topography by using SfM method.

2. New sand bypassing system

Fukude Harbor and Asaba Coast are located in Shizuoka Prefecture in Japan, facing the Pacific Ocean. Asaba Coast is one of the valuable beaches which are used as natural egg-laying site of sea turtle. Sand supply in this area originates from the Tenryu River, which locates about 12 km to the west (Figure 1). However, after the construction of breakwater of Fukude Fishery Harbor in 1979, it interrupted longshore sediment transportation from the west to the east and caused severe coastal erosion on the Asaba Coast, located on the east side of the harbor. Moreover, on the west side and around the entrance of the harbor,

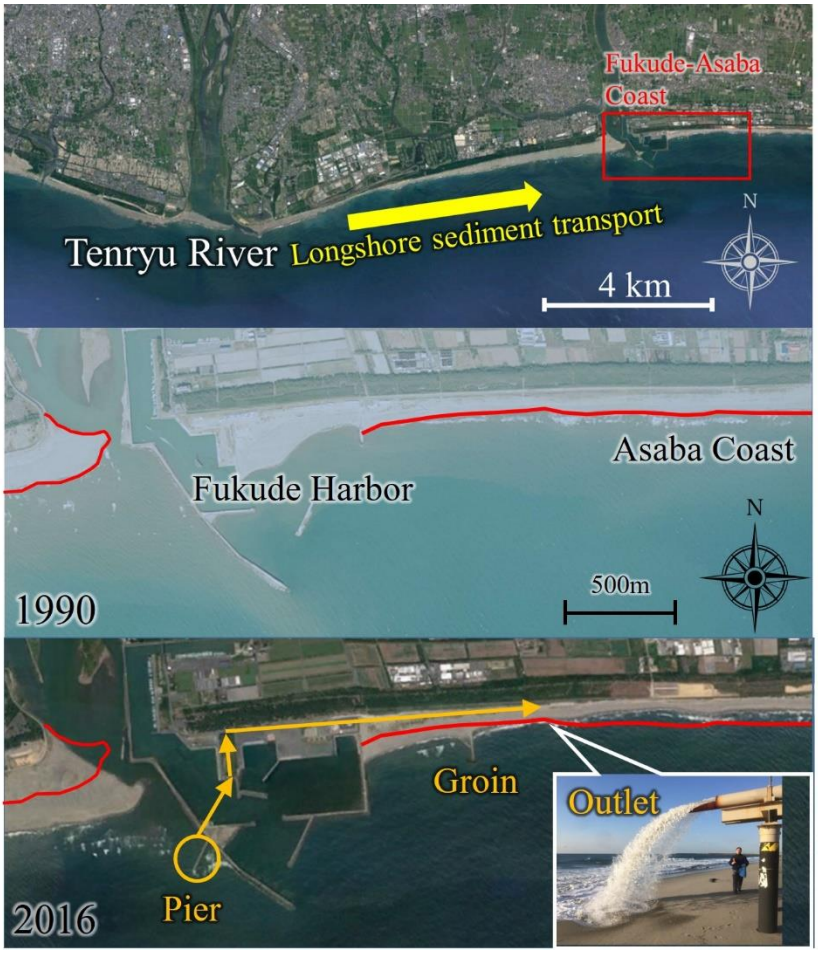

Figure 1. New sand bypassing system installed on Fukude Harbor and Asaba Coast. Red line in middle and bottom figure means shoreline in 1990.

excessive sedimentation caused navigation problems of fishery boats. Figure 1 shows comparison of shoreline change between 1990 and 2016 by using aerial photos. In this figure, red line represents shoreline of 1990. The shoreline has advanced by 150 m on the west side of the harbor while the shoreline has retreated 50 m on the Asaba Coast. In order to mitigate the problem, continuous sand dredging has been conducted around the harbor with dredged sand nourished on Asaba Coast, and a groin was constructed (see Figure 1). In 2015, the government introduced an automated sand bypassing system. In this system, totally about 80,000 m^3/year of sand transportation is designed.

3. Monitoring Methodology

3.1 *Field survey*

Field surveys were conducted on August 2nd in 2015 and January 7th, March 26th, June 29th, and November 3rd in 2016, by using UAV named DJI phantom 2 vision + and DJI phantom 4. Both UAVs can fly almost 25 minutes in one flight with their camera view and altitude simultaneously displayed on the operator's smartphone at hand. The resolution of the former is 4384 x 3288 in snapshot and 1920 x 1080 in video, while the latter is 4000 x 3000 in snapshot and 3840 x 2160 in video. In the field surveys, the bathymetry was estimated through videos taken vertically down to the sea in front of the outlet at a height of 150 m. The subaerial beach topography was estimated through snapshots taken at a height of 30 m with various view angles. Three dimensional topography model was developed by the SfM technique for the 1 km stretch of the beach on both sides of the outlet. Moreover, in the field survey on January 7th, a surveillance camera has been installed at a nearby telegraph pole at the location indicated by a white marker in Figure 2. The camera takes pictures every 2 seconds for one minute in every 30 minutes from 06:00 to 18:00. These pictures were used to monitor the shoreline change.

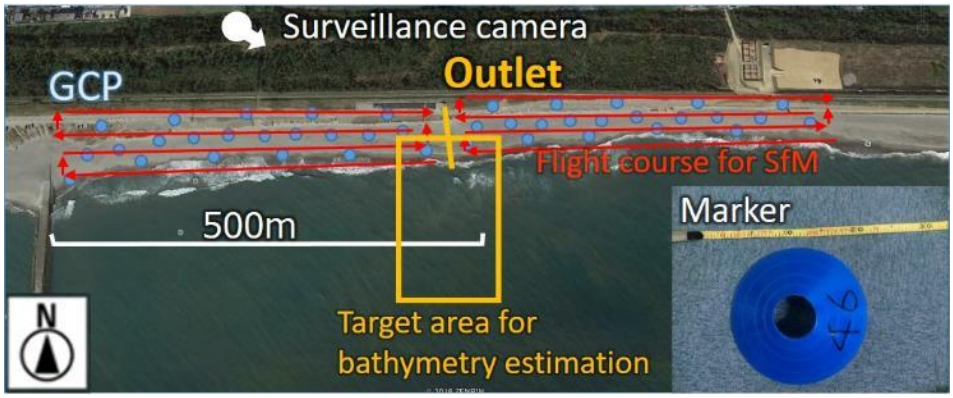

Figure 2. Outline of filed surveys; Red arrows mean flight course of UAV and blue marks represents Ground Control Points put on the beach.

3.2 *Monitoring shoreline change*

By using the pictures taken by the surveillance camera, shoreline change can be monitored. At first, time-averaged pictures were made by using pictures of each interval of 30 minutes based on Lippmann and Holman (1989). Time-averaged picture is a picture obtained by averaging each value of RGB in of the dataset. Figure 3 shows one of the examples of time-averaged pictures. As shown in this figure, in time-averaged pictures, swash zone can be clearly seen in white.

Distortion caused by lens was removed based on Brown (1971), which assumes that the distortion can be approximated as polynomial function of distance from center of the picture with several parameters. After removing the lens distortion from time-averaged pictures, these pictures were converted to rectified pictures with the method proposed by Holland (1997). In order to rectify these pictures, several Ground Control Points on the beach and coordinates of the surveillance camera were used, which were measured with RTK-GPS (Real Time Kinematic GPS) when the camera was installed. Figure 4 shows one of the

Figure 3. Examples of (a) pictures taken by surveillance camera and (b) time-averaged pictures.

results of the rectification of time-averaged picture. The length of one pixel in this picture corresponds to 0.2 meters in the horizontal distance in real. Then, from rectified time-averaged pictures, shorelines were automatically extracted as the local maximum points, which is nearest to the beach, of the gradient of the brightness of the pictures, in the cross-shore direction. In some case where it was difficult to extract shoreline from time-averaged pictures because of calm wave condition, occasional appearance of people and cars on the beach, and so on, the shoreline was extracted manually. The red line shown in Figure 4 is automatically extracted shoreline and blue markers mean several points on the shoreline which were measured with RTK-GPS. These results were compared with shoreline measured with RTK-GPS in January 7th and June 28th in 2017, and averaged error was 0.51 m in cross-shore direction.

3.3 *UAV-based monitoring*

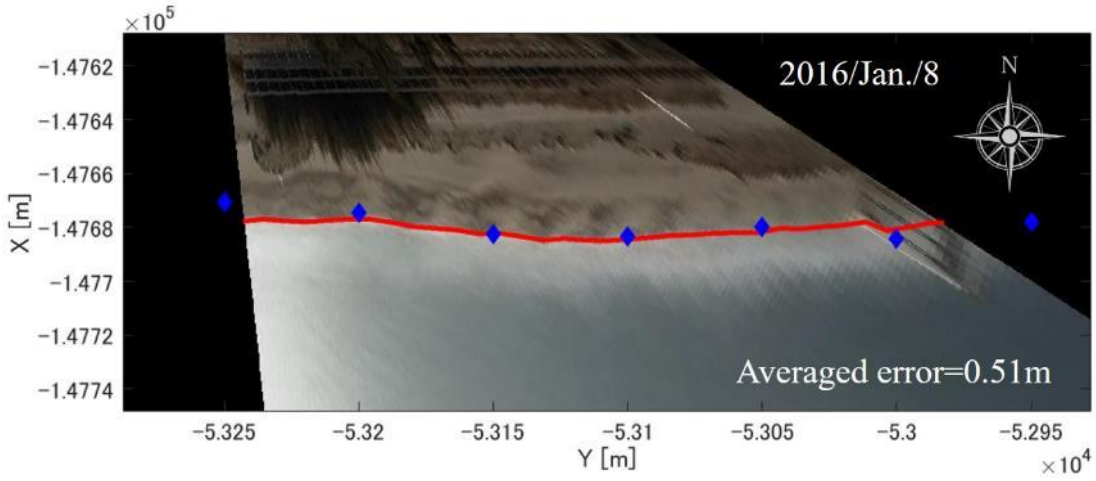

Figure 4. Example of the rectified pictures. Red line shows shoreline extracted automatically and blue markers mean points on shoreline measured with RTK-GPS in the field survey.

3.3.1 *Topography estimation based on SfM.*

SfM (Structure from Motion) is a technique of estimating three dimensional structures from two dimensional image sequences by finding reference points in each pictures. Mancini et al (2013) utilized this technique for monitoring beach topography. In this study, this technique was also applied. At first, almost 40 markers, which were used as Ground Control Points, were situated on the target beach with their geographical coordinates measured by RTK-GPS. Then, pictures with various view angles were taken by UAV with flying around the target area as shown in Figure 3. For constructing three dimensional model, a software named PhotoScan was used, which is developed to apply SfM technique automatically. On this soft, the distortion of each image can be removed based on the same method mentioned before by using the

same parameters used beforehand. However, the former UAV, Phantom 2 vision +, uses wide angle lens and the distortion was so large that only the center of each image (2000 x 2000), where the distortion seems to be small, was used for SfM. Figure 5 shows an example of three dimensional model of the Asaba Coast. Figure 5 shows the comparison of estimated elevation by SfM with topography measured simultaneously by using RTK-GPS. It is confirmed that the estimation by SfM agrees well with GPS measurements. Even though the error cannot be neglected in the run-up area, the overall estimation error was 0.097 m in the median. In this study, the data of the swash zone were removed because they cannot ensure the accuracy.

3.3.2 Bathymetry estimation

Bathymetry estimation based on image analysis has been an important subject in order to realize high resolution and frequent monitoring of coastal morphology with low cost. Stockdon and Holman (2000)

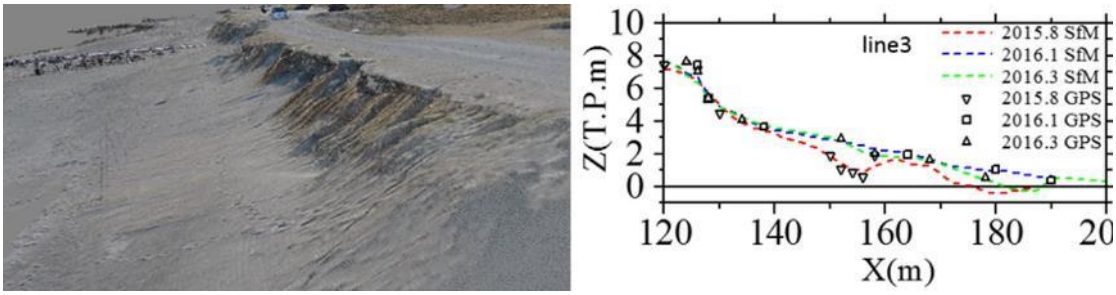

Figure 5. Example of three dimensional model made with SfM technique (left) and Comparison with GPS data (right).

utilized surveillance camera and estimated water depth based on wavenumber obtained by applying CEOF (Complex Empirical Orthogonal Function) for time series of image intensity. Liu et al (2012) monitored long term morphology change in coastal area based on averaged wave celerity given from phase difference of time series of intensity in every points. These methods are inverse depth estimation based on dispersion relation by using average wave celerity. Matsuba and Sato (2017) concluded that the inverse estimation using wave celerity must be applied carefully since the wave celerity only for long period waves can ensure the accuracy. In this study, the inverse depth estimation method proposed by Matsuba and Sato (2017) was utilized with focus on the extraction individual waves with period longer enough for depth estimation and removal of short period waves.

In the field surveys, at first, videos vertical down to the ground were taken by UAV, which hovered at the height of 150 m. The video was separated in every frame with about 0.16 s interval and the lens distortion of each image was removed by the same technique mentioned before. The occasional fluctuation of each frame due to strong wind was adjusted by rotation and displacement based on several blue sheets situated on the beach as the Ground Control Points. After the position correction, all of pictures were converted from RGB to HSV, and then intensity V was utilized for the analysis.

In order to extract wave crest lines in every image, Matsuba and Sato (2017) developed two techniques: one is to focus on brightness distribution in cross-shore direction and the other is to utilize two dimensional wavelet transform. In this study, the latter technique was applied since it has advantage in extracting long wave components. The wavelet transform is a technique to decompose a signal based on differences of frequency by using a basic function called mother wavelet function. The wavelet spectrum is defined as the convolution of discrete sequence and a scaled and translated normalized mother wavelet (Torrence and Compo, 1998). Wavelet transform is given by following equation;

$$W(x_0, y_0, s) = \frac{1}{s}\sum_x \sum_y \psi\left(\frac{x - x_0}{s}, \frac{y - y_0}{s}\right) f(x, y) \tag{1}$$

where W is wavelet transform, f is target matrix, s is scale parameter and ψ is mother wavelet function. In this method, the two dimensional Gabor function was used as the mother wavelet function, which is expressed as a product of the Gaussian function and the sinusoidal function, and is given as the following equation;

$$\psi(x, y) = \frac{1}{2\pi\sigma}\exp\left(-\frac{x'^2 + \gamma^2 y'^2}{\sigma^2} + i(\omega x' + \phi)\right) \tag{2}$$

where σ is the scale of Gauss window, γ is the aspect ratio of the Gaussian function, ω is the wavenumber and ϕ is the phase lead. The coordinate x', y' are defined by the following equation;

$$\begin{pmatrix} x' \\ y' \end{pmatrix} = \begin{pmatrix} \cos\theta & \sin\theta \\ -\sin\theta & \cos\theta \end{pmatrix} \begin{pmatrix} x \\ y \end{pmatrix} \tag{3}$$

where θ corresponds to the direction of wave propagation.

In this extraction technique, at first, the wavelet spectrum is calculated by using Eq. (2) with the scale parameter estimated beforehand based on the target wave length longer enough to ensure the accuracy. Then, the location of wave crest lines can be detected as the local maximum points of wavelet spectra W in the cross-shore direction. Wave crest lines extracted by the wavelet transform include fake/erroneous extraction. Therefore, the removal of them is also required. Propagation of individual extracted waves are traced by searching the identical wave in the next image in the direction normal to the wave crest lines. Then, only wave crest lines whose propagation can be confirmed for longer than 5 s are used for the depth estimation. Figure 6 shows an example of extracted long wave crest lines after the removal of erroneous extractions.

By tracing these wave crest lines as the same method with the removal, wave celerity can be calculated. Then, by using the average wave period T, which is also can be estimated by counting waves in the videos, water depth h can be estimated inversely based on the linear dispersion relation;

$$h = \frac{cT}{2\pi}\tanh^{-1}\frac{2\pi c}{gT} \tag{4}$$

Matsuba and Sato (2017) conducted several field tests of this method and demonstrated that the error was at most 0.3 m in the shallow area on submerged breakwaters. The estimated water depth was used to calculate the bed elevation above the datum by using tide data of Omaezaki measured by the Japan Meteorological Agency.

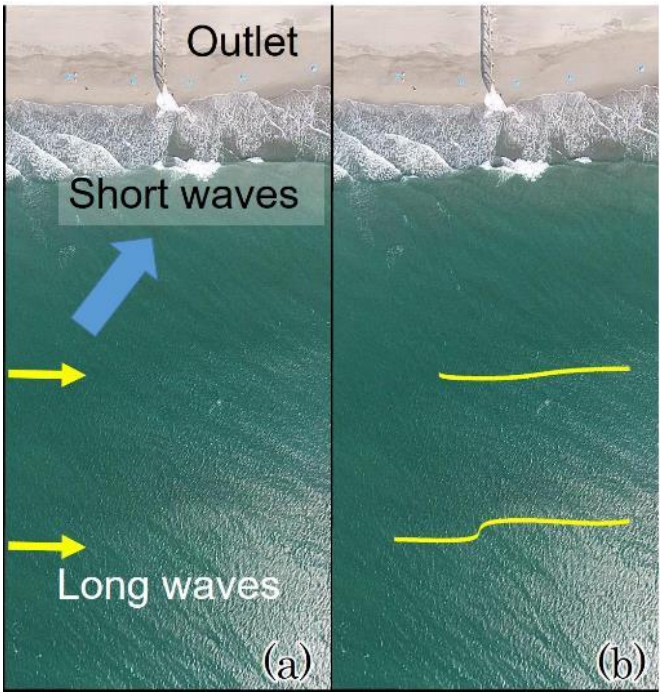

Figure 6. (a) Sample frame taken by UAV and (b) extracted long waves.

3.3.3 Nearshore topography change around the outlet

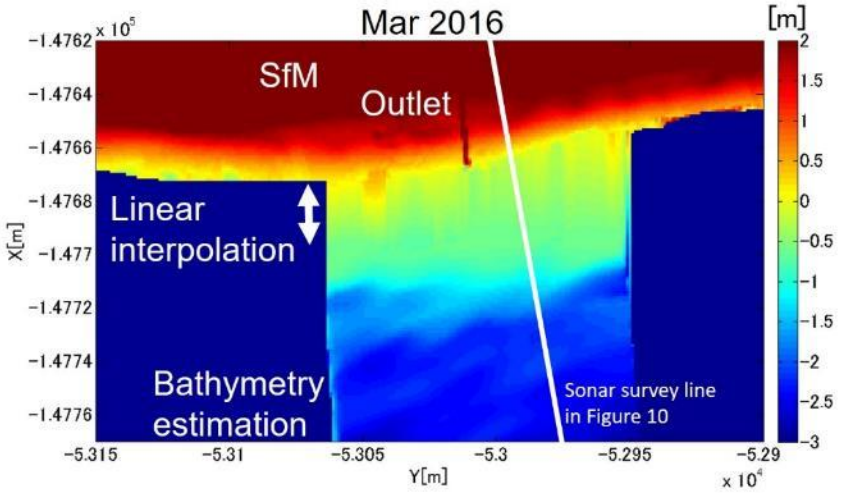

Figure 7. Example of total estimated topography (March, 2016).

By combining subaerial topography estimated based on SfM method and bathymetry estimated inversely, nearshore topography around the outlet was estimated. In these two estimations, it is difficult to estimate the topography of run-up area. Therefore, by using linear interpolation, the two topography data were connected. Figure 7 shows the result of topography estimation of March in 2016.

4. Result

4.1 *Trend captured by shoreline change*

Figure 8 shows the wave climate estimated from data by Ryuyo Observatory, Shizuoka Prefecture, from January to December in 2016. As shown in this figure, the dominant wave direction is from SE, but most of the waves from SE are not large and the number of waves larger than 1 m height are almost same both in SE and SW. Especially from January to March, dominant wave direction is from SW, and the figure suggests that large waves came from SW from July to September, in typhoon season. Therefore, longshore sediment transport from the west to the east will dominate in the end of winter and typhoon season, and the opposite in the spring and after the autumn.

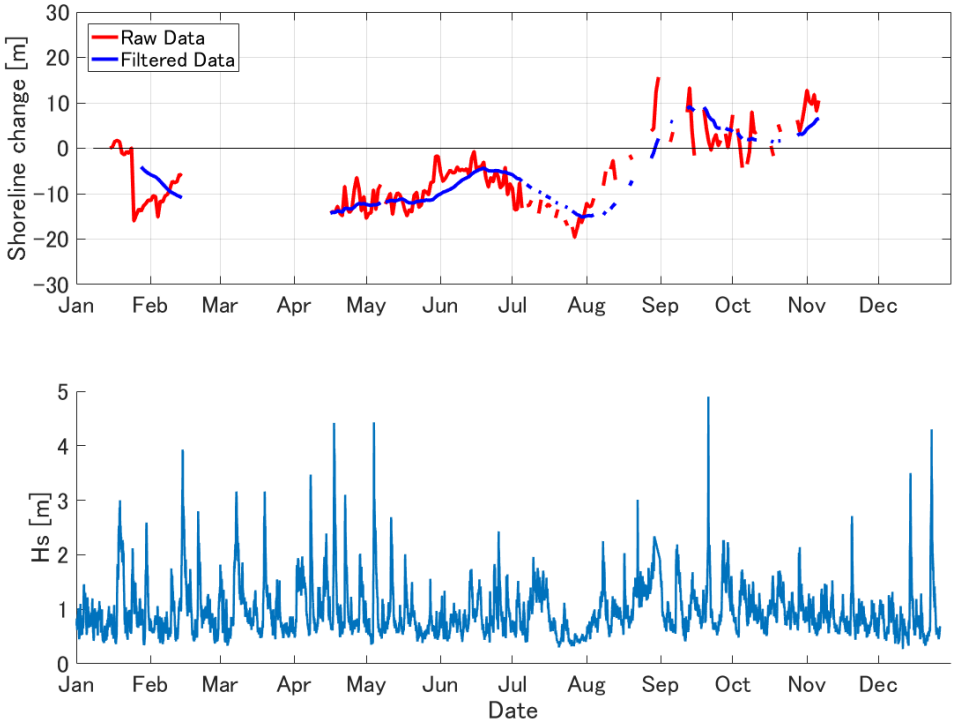

Figure 9. Shoreline change and significant wave height in 2016.

Monitoring shoreline change around the outlet with the surveillance camera was conducted from January 8th to November 3rd including lack of data. Figure 9 shows shoreline change at the outlet as the difference from shoreline in January 8th in cross-shore direction, averaged in longshore direction in the monitored area, and the wave height at Ryuyo Observatory during the period. The positive value means the beach recovery. Red line shows measured variation day by day and blue line shows trend of the variation. A large coastal erosion with 10 m retreat is observed in a month from the beginning. The shoreline retreat remained until the beginning of the spring. This large erosion can be explained as the result of sediment transport from the west to the east caused by several winter storm during the period. The shoreline slightly recovered from June but it turned back to the erosional trend again in summer. These trends must be due to

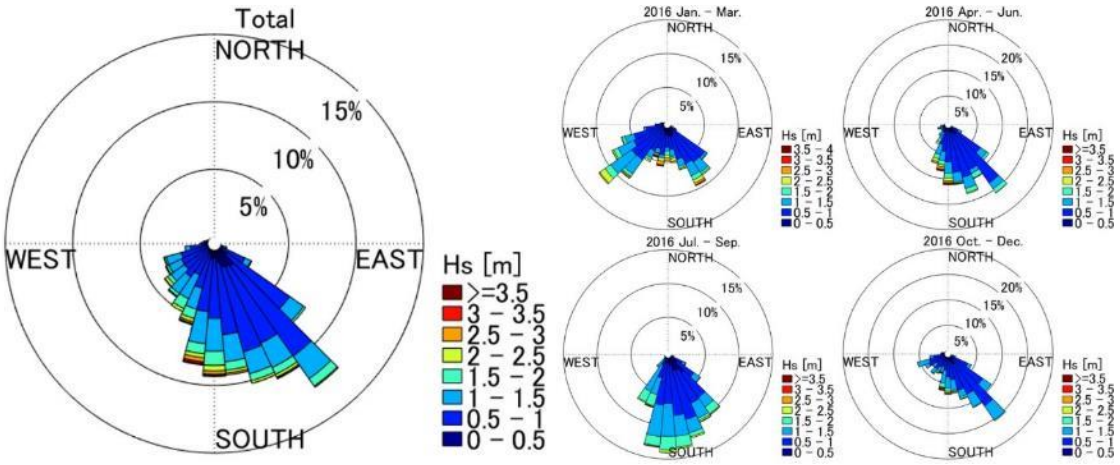

Figure 8. Wave distribution during the monitoring period.

several typhoon attacks. Significant beach recovery is noticed from August, resulting a shoreline advancement as much as 10 m from January to November in 2016. These seasonal shoreline variations are consistent with the longshore sediment transportation estimated by the wave climate.

4.2 *Change of cross-shore profile captured by UAV monitoring*

Based on the UAV based morphology estimation of field surveys, the change of the cross-shore profile is shown in Figure 10 as the colored lines. The profiles are illustrated along the white line in Figure 7, which represents the topography measurement by Shizuoka Prefecture by using sonar sounding. The sonar sounding on May and November in 2015 and February in 2016 are also drawn in Figure 10 as black lines. Before the start of continuous operation of the sand-bypassing system, from May to August in 2015, the beach was eroded a little and sediment accumulated nearshore area. It can be expected several large typhoons caused these sediment transport in the offshore direction. After the start of the operation on October in 2015, large accumulation occurred until November in 2015. This trend continued to January in 2016. Especially on land area and in the trough area behind the longshore bar, large deposition was observed. However, after January large erosion was observed in February because of attacks of large winter storm as mentioned before. Even though the winter storms left huge impacts on morphology change, the depositional trend was continuously observed from March to November in 2016. The trend is consistent

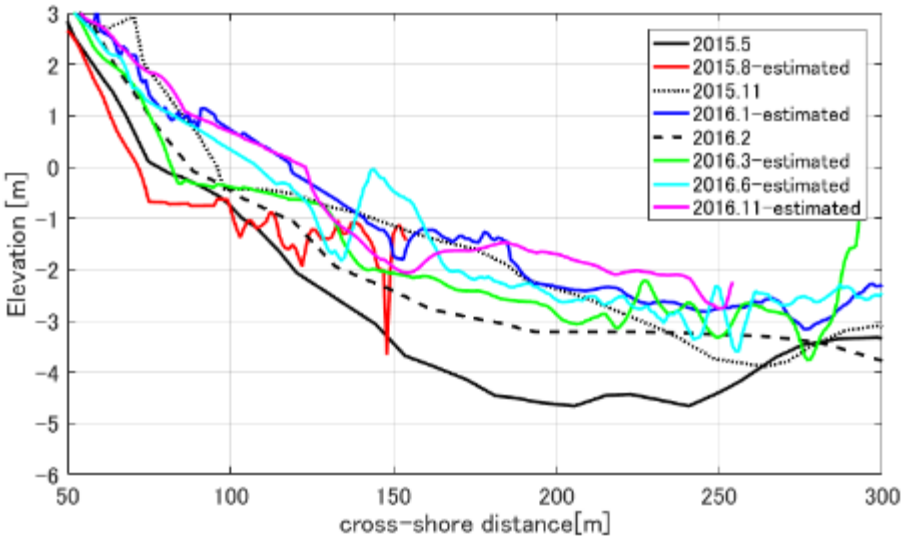

Figure 10. Cross-shore profile on the white line in Figure 7 from August 2015 to November 2016.

with that in shoreline changes captured by the surveillance camera.

4.3 *Spatial distribution of morphology change estimated by UAV*

Figure 11 shows difference of estimated morphology distribution captured by UAV on August 2nd in 2015, January 7th, March 26th, June 29th, and November 3rd compared with one of previous field survey and total net difference in about one year (from January to November). The estimated area on August 2nd was smaller than the others because the target area then was narrower than the others. Therefore, it is impossible to compare in whole area, however, large accumulation was observed from August in 2015 to January in 2016, especially on the western side of the outlet. Total increase of the sand volume in the area shown in Figure 11 during the period was estimated as about 1.9×10^4 m^3, which was about 45% of the bypassed sand volume in the period. From January to March, severe erosion was observed with formation of a wide step close to the shoreline. After the large erosion in winter season, significant deposition was found from March to November. Even though a little erosion was observed from March to June near from the shoreline, the UAV-based system revealed overall recovery trend. In one year from January to November in 2016, even though slight erosion was observed in front of the outlet on the sea bottom, total sand volume increased as 3.2×10^3 m^3, especially on the subaerial beach (see Figure 11).

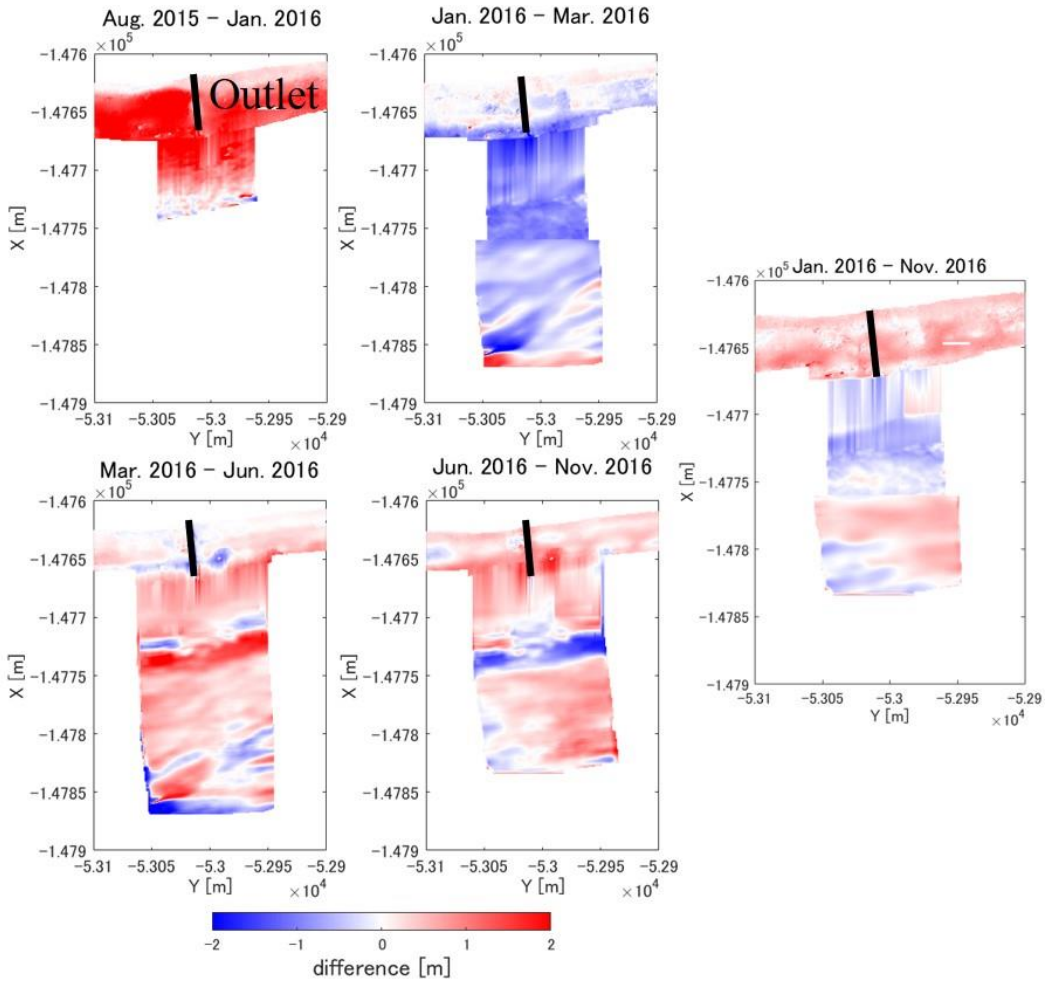

Figure 11. Net difference between two continuous field surveys (left) and in about one year (right).

5. Conclusion

A new UAV-based monitoring system was developed and applied to the Asaba Coast, where the outlet of the pipeline-based sand-bypassing system was installed in 2015. Field surveys using UAV were conducted in each season before the start of the continuous operation in October in 2015 to November in 2016, and the supplementary monitoring by surveillance cameras was carried out from January to November in 2016. Monitoring by the surveillance camera revealed significant shoreline retreats in winter season caused by seasonal storms together with rapid beach recovery after summer. The shoreline advancement at the outlet of the sand bypassing system reached about 10 m in one year.

The new UAV based monitoring system was developed by combining two techniques: SfM method using snapshots taken by UAV and submarine bathymetry estimation by following wave propagation captured by UAV. The SfM method was found applicable to measure subaerial topography in the target area extending about 1 km alongshore. Validation of this method was conducted by comparing with GPS measurements with estimation error smaller than 0.1m. Bathymetry estimation was conducted by following previous study and by extracting only long waves, which ensure the accuracy in the depth inversion, by using 2-D wavelet transform. By applying these techniques, a large and rapid topography change was observed around the outlet of the sand-bypassing system. Especially after the start of continuous operation, about 1.9 x 10^4 m^3 of sand was accumulated around the outlet for about 3 months, which corresponds to 45% of the bypassed sand volume. Significant beach erosion was observed by winter storms although the

erosion is followed by the recovery trend in both subaerial and submarine areas. Further study will be carried out in a wider and longer scales, to understand the beach response due to the sand-bypassing.

References

Brown, D. C. 1971. Close-range camera calibration. *J. Amer. Soc. Photogrammetry*, 37: 855–866.

Holland, K. T., Holman, R. A., Lippmann, T. C. 1997. Practical use of video imagery in nearshore oceanographic field studies. *J. Oceanic Eng.*, 22(1): 81-92.

Inukai, N., Ejiri, Y., Ootake, T., Yamamoto, H., Hosoyamada, T. 2015. A study for the generation on mechanism of the rip current at the enclosed beach by the groin. *J. JSCE*, Ser. B3(Ocean Engineering), 71(2): I_1191-I_1196.

Lippmann, T. C. and Holman, R. A. 1989. Quantification of sand bar morphology: a video technique based on wave dissipation. *J. Geophys. Res.*, 94(C1): 955-1011.

Liu, H., Arii, M., Sato, S., Tajima, Y. 2012. Long-term nearshore bathymetry evolution from video imagery: a case study in the Miyazaki Coast. *Coastal Eng. Proc.*, 1, doi: 10.9753/icce.v33.sediment.60

Mancini F, Dubbini M, Gattelli M, Stecchi F, Fabbri S, Gabbianelli G. 2013. Using Unmanned Aerial Vehicles (UAV) for High-Resolution Reconstruction of Topography: The Structure from Motion Approach on Coastal Environments. *Remote Sensing*, 5(12): 6880-6898.

Matsuba, Y. and Sato, S. 2017. Nearshore bathymetry estimation using UAV. *Coast. Eng. J.*, in submission.

Stockdon, H. F. and Holman, R. A. 2000. Estimation of wave phase speed and nearshore bathymetry from video imagery. *J. Geophys. Res.*, 105(C9): 22015-22033.

Torrence, C. and Compo, G. P. 1998. A practical guide to wavelet analysis. *Bulletin of the American Meteorological Society*, 79(1): 61-78.

TWEED SAND BYPASSING. http://www.tweedsandbypass.nsw.gov.au/, Accessed at March 29, 2017.